

Design of Miniaturized Frequency Selective Surfaces Using Minkowski Island Fractal

Antonio Luiz P. S. Campos and Elder Eldervitch C. de Oliveira

Federal University of Rio Grande do Norte, Department of Communication Engineering, Av Sen Salgado Filho, S/N, Lagoa Nova, 59072-970 Natal, RN, Brazil. e-mail: antonio.luiz@pq.cnpq.br

Paulo Henrique da Fonseca Silva

Federal Institute of Education, Science and Technology of Paraíba, Group of Telecommunications and Applied Electromagnetism, Av. Primeiro de Maio, 720, Jaguaribe, CEP 58015-430, João Pessoa, PB, Brazil. e-mail: henrique@ifpb.edu.br

Abstract— This paper presents a simulation and experimental investigation of a frequency selective surface (FSS). The design is achieved by using the Minkowski island fractal. Two structures were designed with Minkowski island fractal level 1 and 2, which act as stop-band filters with resonant frequencies of 9 GHz and 10 GHz, respectively. Both simulation and experimental investigations were conducted. Simulation investigation was carried out using Ansoft Designer™ software, while experimental investigation used an Agilent Technologies vector network analyzer – model N5230A.

Index Terms— Frequency Selective Surfaces, Stop-band filter, Minkowski fractal.

I. INTRODUCTION

Frequency Selective Surfaces are two-dimensional arrays of periodic metallic elements on a dielectric layer or two-dimensional arrays of apertures within a metallic screen. They are used for a variety of applications, such as bandpass radomes for missiles, sub-reflectors for dual frequency reflector systems, microwave, optical, and infrared filters etc. [1] – [3].

FSS with fractal elements has attracted the attention of microwave engineering researchers because of its attractive features. Several fractal iterations can be used to design an FSS with multiband frequency response associated to the geometry scales contained in the structure. The Sierpinski fractal was previously used to design a multiband FSS [4] – [5].

An experimental investigation was performed by Sarkar *et al.* in [6]. This investigation showed that the reflection bandwidth was very narrow. The authors used dual-frequency resonance within the same frequency band to broaden the reflection bandwidth. A technique for designing multiband frequency selective surfaces using fractal screen elements was proposed in [7].

The design, simulation, fabrication and measurement of pre-fractal surfaces were discussed in [8]. The simulation methods developed for complex periodic structures were used to analyze the structures and were verified with the measured results. The measurement techniques to acquire the frequency and angular responses were also covered.

There are a number of published studies on the use of Minkowski curves to design absorbers and

EBG filters [9], [10]. However, in our opinion, these studies used the Koch curve and not the Minkowski curve, as evidenced in [11] and [12]. Furthermore, these studies ([9] and [10]) focus on absorbers and EBG filters, respectively. This paper investigates FSS using Minkowski curves.

There are several methods to theoretically analyze the different types of FSS structures, but only three methods are widely used: the Finite Difference Time Domain (FDTD) method, Finite Element Method (FEM), and the Method of Moments (MoM). Different types of software are available for theoretical analysis using different methods. CFDTD software provides theoretical analysis for the FDTD method; HFSS software is used for theoretical analysis of an FSS structure using FEM. Ansoft Designer™ uses the MoM to perform theoretical analysis of FSS structures.

In this paper, FSS structures with the Minkowski island fractal were theoretically analyzed by Ansoft Designer™ software and the results compared with experimentally measured data. A great advantage of Minkowski fractal shape is that it is easy to approximate by the rectangular grid used in most full wave electromagnetic simulators.

II. FRACTAL STRUCTURES AND RESULTS

The generation of the Minkowski island fractal is carried out using a recursive procedure, which is characterized by two fractal parameters: iteration number (or level) and iteration factor. From the initiator square at each recursion, an 8-side generator is applied to the pre-fractal at the previous iteration. For the Minkowski fractal, the iteration factor ($1/r$) is four and the number of copies (N) is eight. Thus, at a given iteration, the Minkowski island perimeter is duplicated, but its area remains the same. The fractal dimension, $D = \log(N)/\log(1/r)$, is 1.5.

The Lindenmayer system (or L-system) and turtle algebra [12] are used to generate and visualize the Minkowski fractals shown in Fig. 1. For this particular case we used an iteration factor equal to $1/4$ of the segment.

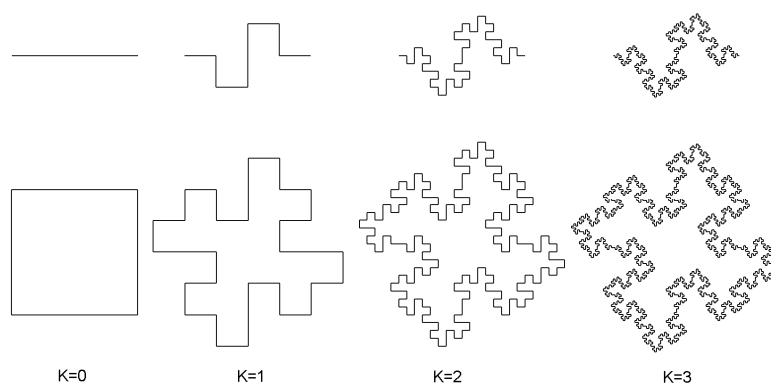


Fig. 1. Minkowski sausage and Minkowski island fractal iterations for levels $K=0, 1, 2, 3$.

The components of an L-system are: (i) alphabet, which is a finite set V of symbols, usually taken to be letters or possibly some other characters; (ii) axiom (or initiator), a string w of symbols from V ; (iii) and production (or rewriting rule), a mapping of a symbol $a \in V$ to a word $w \in V^*$, symbolized by

$p:a \rightarrow w$, where v^* denotes the set of strings (or words) from v . Using the L-system notation results $w =$ 'F' (straight-line initiator) for the Minkowski sausage and $w =$ 'F+F+F+F' (square initiator) for the Minkowski island; $p:'F' \rightarrow 'F+F-F-FF+F+F-F'$ for both Minkowski fractals. From the graphic interpretation of strings based on turtle geometry, a state of the turtle is defined as a triplet (x, y, α) , where (x, y) is the turtle's position, and α is the angle associated to the direction in which the turtle is facing. For the Minkowski fractals illustrated in Fig. 1, the turtle responds to the commands represented by the symbols: 'F' move forward, '+' turn left 90° , and '-' turn right 90° . Fig. 2 illustrates a cell of the proposed structures with its dimensions in mm. The structures are totally symmetric and the same behavior is observed for vertical and horizontal polarization.

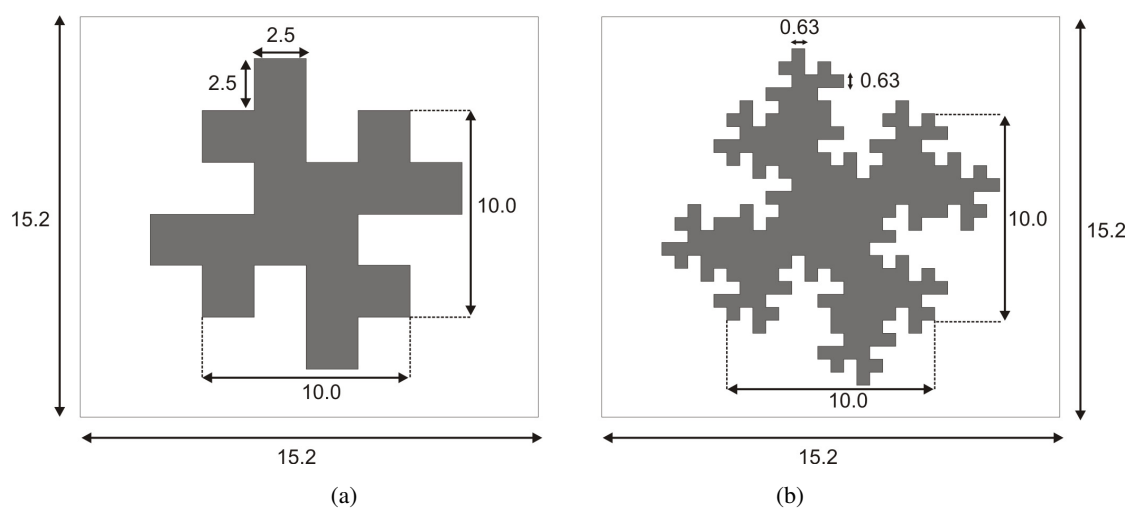


Fig. 2. Unit cell of the Proposed FSSs: (a) Level 1 and (b) level 2.

The periodic arrays of Minkowski FSSs were mounted on a dielectric isotropic layer. The substrate used was the RT-Duroid 3010, with a height of 1.27 mm and relative permittivity of 10.2. The distance between the centers of any two adjacent patches is 15.2 mm. The fabricated FSS can be seen in Fig. 3.

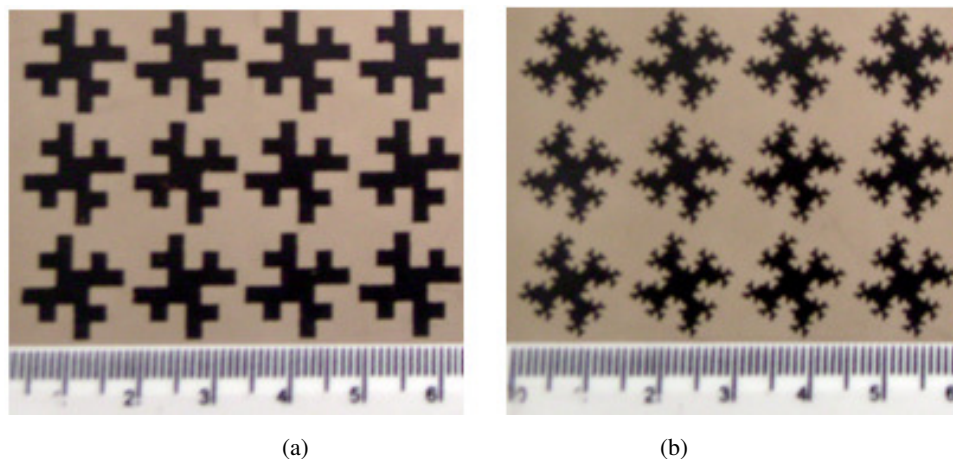


Fig. 3. Minkowski sausage and Minkowski island fractal iterations for levels $K=0, 1, 2, 3$.

We simulated the FSSs in Ansoft DesignerTM software. The proposed structures were arranged in a periodic array, in which a normal incident plane wave was considered, preserving the far-field condition for analysis of the structure investigated. A vertical polarization was considered for the incident wave. Minkowski fractal level 1 FSS obtained a resonance frequency of 9.84 GHz with a – 10 dB bandwidth of 797 MHz. With Minkowski fractal level 2 FSS, we obtained a resonance frequency of 9.00 GHz with a – 10dB bandwidth of at 670 MHz. We can observe a decrease in resonant frequency, whereas the bandwidth showed little change when the fractal level increased. At resonant frequency the rejection was close to 35 dB for the two structures.

After the simulations, FSS fractal level 1 and 2 were fabricated to validate the simulated results. The measurement setup is shown in Fig. 4. To measure the FSS transmission coefficients we used two horn antennas, two waveguides with cutoff frequency of 6.8 GHz, and an N52305 network analyzer (Agilent Technologies). A fixed distance was adopted between the horn antennas to guarantee the operation in the far-field region. This type of measurement setup is listed in [2].

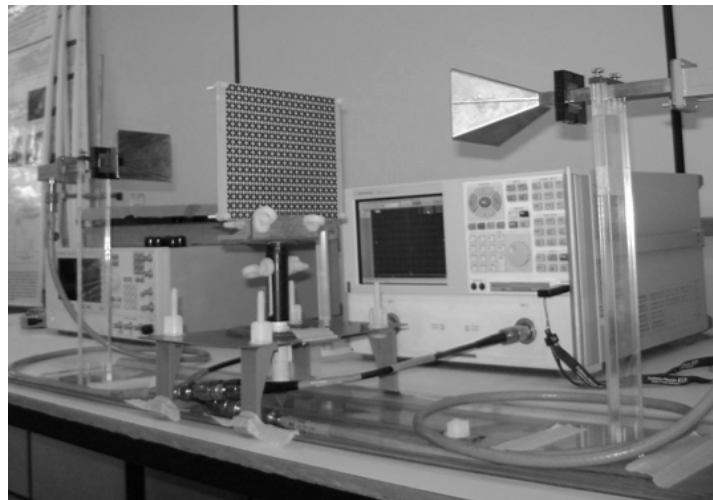


Fig. 4. Measurement setup.

Fig. 5 and Fig. 6 show the simulated and measured results, respectively, for the fabricated FSS. Good agreement can be observed. The results are summarized in Table 1. Resonance frequency and bandwidth errors were less than 1% and 6%, respectively.

TABLE I. COMPARISON BETWEEN SIMULATED AND MEASURED RESULTS

Parameter		Level 1	Level 2
f_r (GHz)	Simulated	9.61	9.00
	Measured	9.84	8.91
BW (MHz)	Simulated	797	670
	Measured	805	635

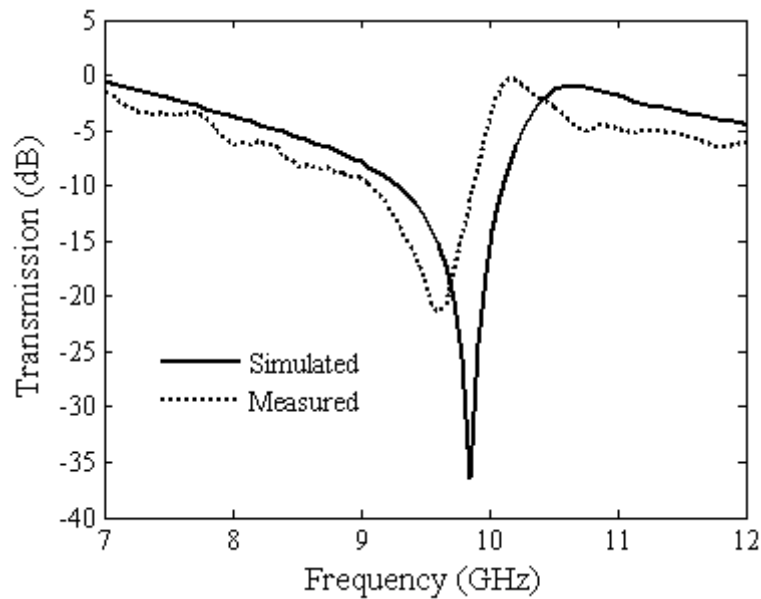


Fig. 5. Comparison between measured and simulated results for Minkowski fractal level 1.

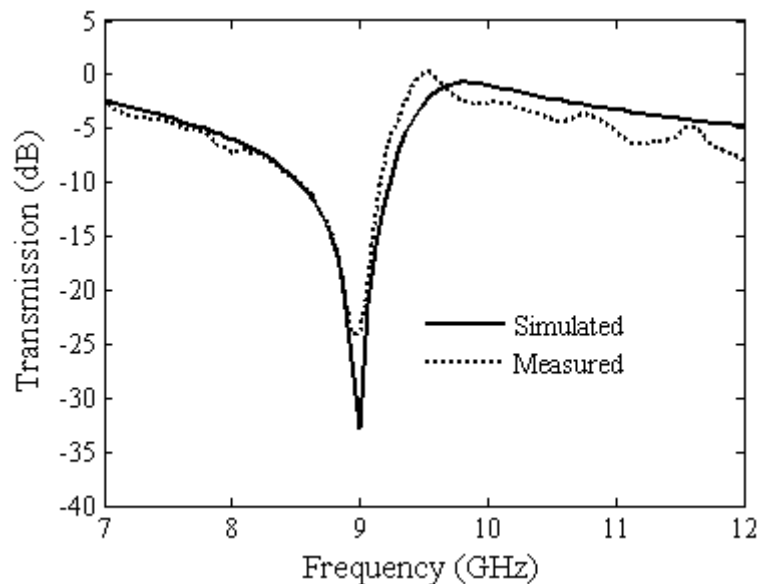


Fig. 6. Comparison between measured and simulated results for Minkowski fractal level 2.

To compare size reduction, we designed two FSS with square patches to operate at frequencies of 9 GHz and 10 GHz. Fig. 7 shows the measured results for Minkowski fractal level 1 FSS and the square patch FSS. The side length of the conducting square patch is 10 mm and periodicity in the x and y directions, is 19.5 mm. For the same resonance frequency, the bandwidth was much smaller than that of the square patch FSS. Fig. 8 illustrates the measured results for Minkowski fractal level 2 FSS and the simulated results for the square patch FSS. The side length of the conducting square patch is 10 mm and periodicity, in the x and y directions, is 22 mm. Again, we can see the same reduction in bandwidth for the square patch FSS. Numerical results were obtained using full wave analysis of the Moment Method.

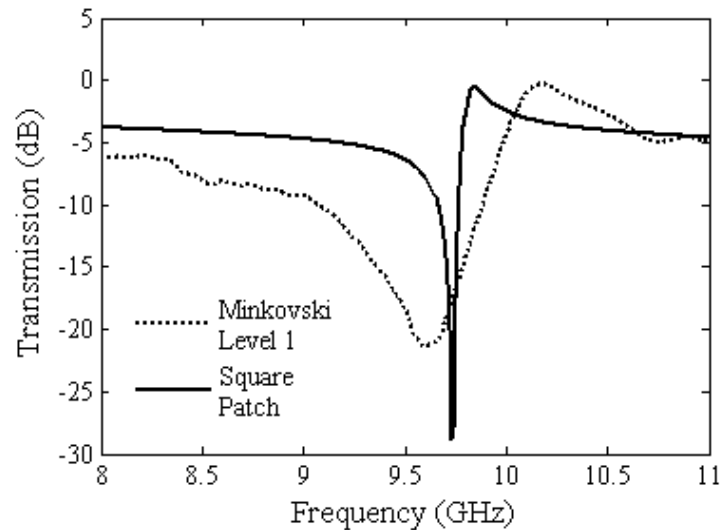


Fig. 7. Comparison between measured results for Minkowski fractal level 1 and numerical results for a square patch FSS.

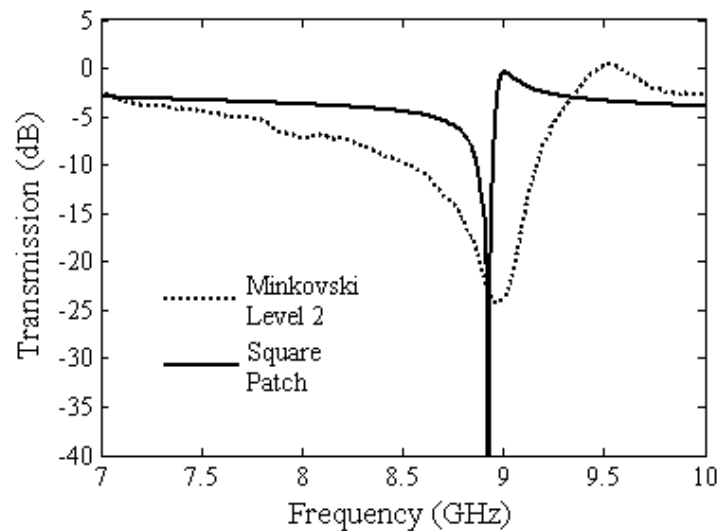


Fig. 8. Comparison between measured results for the Minkowski fractal level 2 and numerical results for a square patch FSS.

III. CONCLUSIONS

In this paper, the use of the Minkowski island fractal was investigated for the design of frequency selective surfaces. A single substrate was used to generate stop-band characteristics. The validity of the simulation results was shown by careful experimentation. Prototypes were fabricated and tested in a free-space environment for different levels of Minkowski curves. Good agreement between the simulations and experimental results was shown. We should note that the use of the Minkowski island fractal in FSS enables a reduction in the unit cell and in the metallic area. The Minkowski fractal element exhibited a bandwidth at -10 dB below 1 GHz, and for some applications this narrow bandwidth may be ideal. Compared with a square patch FSS, the bandwidth obtained with the Minkowski fractal elements were larger, with a 36% reduction in unit cell area for fractal level 1 and 52.3 per cent for fractal level 2.

ACKNOWLEDGMENT

The authors express their sincere thanks to Conselho Nacional de Desenvolvimento Científico e Tecnológico (National Council for Scientific and Technological Development) - CNPq- for supporting this research (project no. 470404/2007-8).

REFERENCES

- [1] J. C. Vardaxoglou, *Frequency-Selective Surfaces: Analysis and Design*. Taunton, U.K.: Res. Studies Press, 1997.
- [2] T. K. Wu, *Frequency-Selective Surface and Grid Array*. New York: Wiley, 1995.
- [3] B. A. Munk, *Frequency-Selective Surfaces: Theory and Design*. New York: Wiley, 2000.
- [4] J. Romeu and Y. Rahmat-Samii, Dual band FSS with fractal elements, *Electronic Letters*, Vol. 35, No. 9 (1999), 702–703.
- [5] J. Romeu and Y. Rahmat-Samii, Fractal FSS: a novel dual-band frequency selective surface, *IEEE Transactions on Antennas and Propagation*, Vol. 48, No. 7 (2000), 1097–1105.
- [6] P. P. Sarkar *et al.*, Experimental investigation of the frequency-selective property of an array of dual-tuned printed dipoles, *Microwave and Optical Technology Letters*, Vol. 31, No. 3 (2001), 189-190.
- [7] D. H. Werner and D. Lee, A design approach for dual-polarized multiband frequency selective surfaces using fractal elements, *IEEE Antennas and Propagation Society International Symposium*, 2000, Vol. 3, No. 3 (2000), 1692 – 1695.
- [8] J. P. Gianvittorio, J. Romeu, S. Blanch, and Y. Rahmat-Samii, Self-Similar Prefractal Frequency Selective Surfaces for Multiband and Dual-Polarized Applications, *IEEE Transactions on Antennas and Propagation*, Vol. 51, No. 11 (2003), 3088 – 3096.
- [9] Y. Lou, Y. Zhuang, and S. Zhu, Thin and broadband Salisbury screen absorber using Minkowski fractal structure, *Microwave Conference Asia Pacific, PMCM 2009*, pp. 2573-2576.
- [10] M. F. Karim, A. B. Yu, A. Alphones, and A. Q. Liu, Fractal CPW EBG Filter with Nonlinear distribution, *Microwave Conference Asia Pacific, PMCM 2005*, Vol. 3.
- [11] E. E. C. de Oliveira, P. H. da F. Silva, A. L. P. S. Campos, and S. G. da Silva, Overall Size Antenna Reduction Using Fractal Elements, *Microwave and Optical Technology Letters*, Vol. 51, No. 3 (2009), 671 – 675.
- [12] J. Mishra and S. Mishra, *L-Systems Fractals*. Amsterdam, The Netherlands: Elsevier, 2007.